

# Mach cone in a shallow granular fluid

Patrick Heil, E. C. Rericha\*, Daniel I. Goldman, and Harry L. Swinney†

Center for Nonlinear Dynamics and Department of Physics, University of Texas, Austin, Texas 78712

(Dated: March 23, 2022)

We study the V-shaped wake (Mach cone) formed by a cylindrical rod moving through a thin, vertically vibrated granular layer. The wake, analogous to a shock (hydraulic jump) in shallow water, appears for rod velocities  $v_R$  greater than a critical velocity  $c$ . We measure the half-angle  $\theta$  of the wake as a function of  $v_R$  and layer depth  $h$ . The angle satisfies the Mach relation,  $\sin \theta = c/v_R$ , where  $c = \sqrt{gh}$ , even for  $h$  as small as one particle diameter.

The interactions of a flow with an obstacle have been a test bed for fluid mechanics throughout the past century [1]. For example, measurements on the Von Kármán vortex street of flow past a cylinder, the drag force reduction due to turbulence, and shock wave interactions with airplanes continue to increase our understanding of fluid mechanics. Experiments on granular flow past obstacles provide good geometries to test the emerging hydrodynamic theory [2, 3, 4, 5, 6, 7, 8] for rapid granular flows. In addition, studying the interaction of granular flows and obstacles is important for industrial applications. Obstacles are often introduced to modify granular flows: paddles are used to mix materials; inserts are added to granular bins to reduce stresses; and pipes are inserted in chute flows as heat transfer surfaces [9].

Measurements on experimental and simulated flow fields indicate that shocks commonly develop when granular flows interact with obstacles [6, 10, 11, 12, 13]. Shocks form when the relative velocity between an obstacle and a fluid exceeds the wave speed in the medium. The shock front is a superposition of waves excited as the obstacle moves through the fluid. For a dispersionless Newtonian fluid with a constant wave speed, the front coalesces into a Mach cone with a half angle given by the Mach relation,

$$\sin \theta = \frac{c}{v_R}, \quad (1)$$

where  $c$  is the wave speed and  $v_R$  is the obstacle's velocity. Experiments and simulations on shocks in granular flow have not revealed an analogous relationship between  $v_R$  and the shock angle.

We study a phenomenon that is the analog of a compression shock: the wake that forms behind an obstacle moving on a free surface of a fluid layer. We measure the height field behind a thin rod moving through a vertically vibrated granular layer. We find the wake angle follows the Mach relation (1) and is well described by the shallow water theory for fluid flows without surface tension. In this theory, the description of the wake is

identical to that of a compressible shock in a dispersionless gas. Thus, the wake formed in the thin granular layer can be described by the usual tools of shock physics.

*Experiment:* A stainless steel rod of diameter  $D=0.75$  mm is inserted into a shallow, vibrofluidized granular layer consisting of bronze spheres with a diameter  $d = 0.17$  mm. The rod moves in a circular path of radius 51 mm with a constant speed  $v_R$  in the range 4-30 cm/s.

The granular layer is vibrofluidized using an apparatus similar to the one described in [14, 15]. For each layer depth  $h$ , the peak plate acceleration  $2.2g$  and the nondimensional frequency  $f^* = f\sqrt{h/g} = 0.39$  are chosen such that the layer is fluidized but remains below the onset of patterns [16]. The container is evacuated to less than 4 Pa to reduce air effects [17]. The distance from the bottom of the container to the rod is held fixed at  $0.5h$  throughout the container oscillation.

We measure the time-averaged height field of the layer behind the rod using a laserline technique similar to the one reported in [18]. A thin vertical laser sheet (1 mm thick) illuminates the granular layer. When the rod passes through the laser line it triggers a CCD camera, held at a fixed angle with respect to the flat surface. The camera captures 52 digital images of the laser line separated in time by  $\delta\tau = 2.2$  ms (Fig. 1). For  $v_R = 21.5$  cm/s, the distance between line scans is  $v_R\delta\tau = 0.47$  mm. Deviations from a straight laser line indicate the variations of surface height. The resulting height field is shown in Fig. 1.

The height field was averaged over many cycles with the frequency of the driving and rod rotation incommensurate. High speed imaging showed that the angle of the shock front is independent of phase during the driving cycle. The high speed images also showed that the oval peak behind the rod (Fig. 1) is related to the vibration of the layer during the cycle.

*Results:* For small  $v_R$ , the time-averaged layer remains everywhere flat to within our experimental error. For  $v_R$  greater than a critical velocity  $c$ , the height field shows a bow shock structure: a rapid increase in surface height, analogous to a hydraulic jump, develops in front of the rod and extends downstream in a V-shaped wake (Fig. 1). The height profile taken along the dashed line in Fig. 1(b) is shown in the inset of Fig. 2. The increase in height from

\*Electronic Address erin@chaos.utexas.edu

†Electronic Address swinney@chaos.utexas.edu

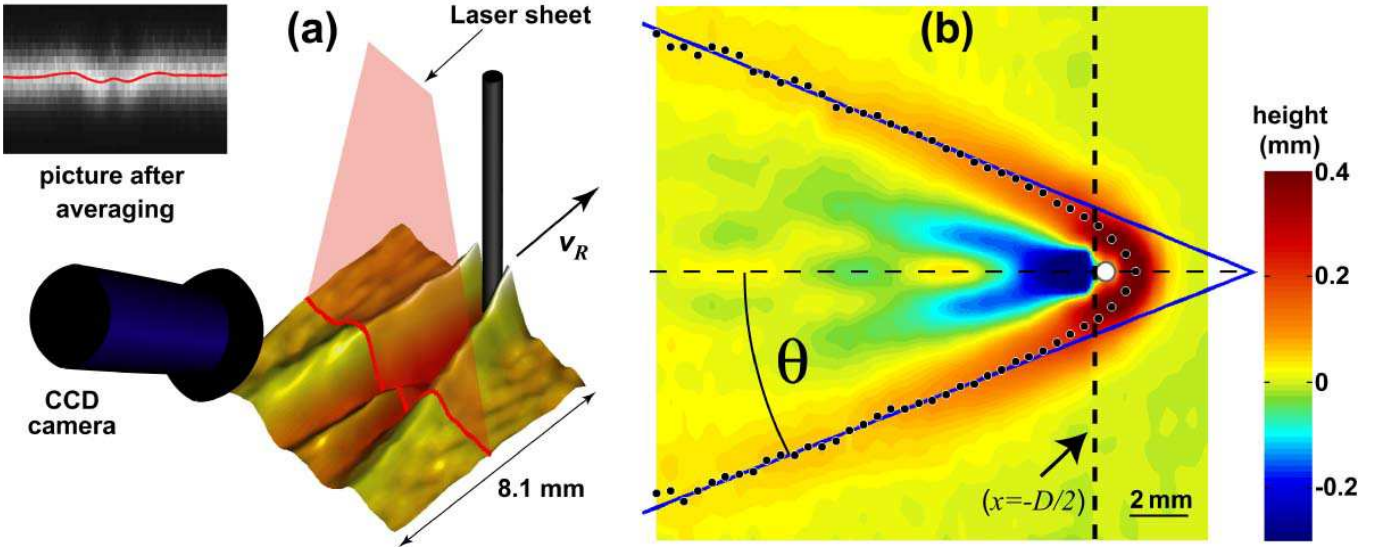


FIG. 1: (color online)(a) Schematic of the laser line scanning technique used to measure the displacement of the surface created by a rod moving through a granular layer. A laser light sheet is incident downward onto the granular layer and is imaged by a CCD camera set at a fixed angle with respect to the surface. The inset shows an image averaged over 400 periods of the rod motion. The location of the laser line is determined to subpixel accuracy by finding the center of a Gaussian fit to each peak in the vertical slice, as shown in the inset (red line). (b) Top view of the shock created by the rod, moving to the right, for  $v_R = 21.5$  cm/s. The location of the maximum layer height  $\Delta h_{max}$  for each scan line is indicated by the dots. A linear fit to the maxima (blue line) yields the wake's asymptotic half angle  $\theta$ . A surface height profile taken along the vertical dashed line is shown in the inset of Fig. 2.

the flat layer to the maximum upward deflection of the layer ( $\Delta h_{max}$ ) measured from the laser line at  $x = -D/2$  directly behind the rod is shown in Fig. 2. For  $v_R > c$ ,  $\Delta h_{max}$  increases linearly with rod velocity. A fit to the data for a layer depth of  $h=4d$  indicates a critical wave speed  $c = 8.4 \pm 0.7$  cm/s [31].

The transition from the subcritical flow without a shock, to a supercritical flow with a bow shock is not sharp, as indicated by the rounding of the transition seen in Fig. 2. As the flow accelerates around the rod, a small supercritical region develops for  $v_R$  less than but near  $c$ . A shock forms in this region, but does not extend out into the fluid.

We measure the half-angle  $\theta$  of the shock with respect to the axis of the rod's motion as a function of  $v_R$ . We define the location of the shock by the maximum of the height field for each line scan. Near the rod the shock is curved; however, within a few rod diameters the shock straightens, creating a V-shaped wake with a well-defined half-angle. A linear fit through the maxima of the asymptotic shock yields  $\theta$  (Fig. 1). We find  $\theta$  is described well by the Mach relation (1) for a compressible gas. The linear dependence of the data plotted in Fig. 3 indicates a constant surface wave speed. For  $h = 4d$  we find  $c = 7.9 \pm 0.4$  cm/s, which is consistent with the critical speed determined from the height measurement.

*Shallow water theory:* Our results can be understood in terms of a shallow water approximation, similar to the approach applied to avalanches [19, 20] and granular

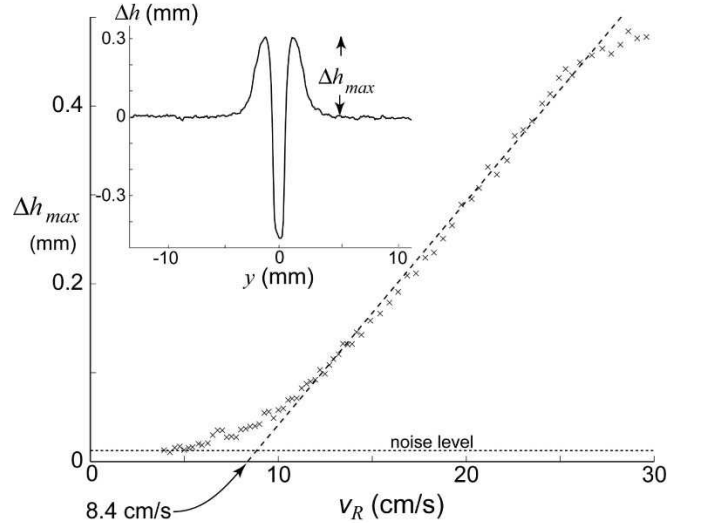


FIG. 2: The maximum upward displacement of the layer  $\Delta h_{max}$  for the line scan at  $x = -D/2$  for (inset shows profile for  $v_R = 23$  cm/s) as a function of  $v_R$  for a layer depth of  $h=4d$ . For small  $v_R$  the layer behind the rod remains flat to within experimental accuracy (dotted line). Above a critical velocity the deflection increases linearly with  $v_R$  (dashed line). The intersection of the dashed line with the horizontal axis indicates a nonzero critical velocity. The noise level was determined by the peak to peak oscillations in the flat part of the layer.

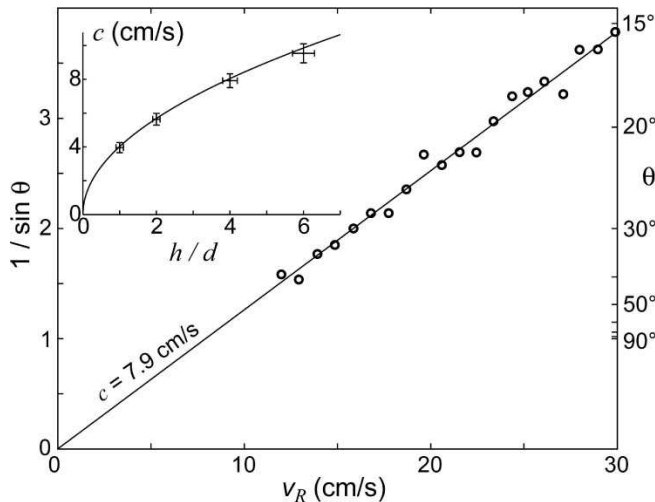


FIG. 3: The measured dependence of the half angle  $\theta$  of the shock cone on  $v_R$  is in accord with the Mach relation (1) (solid line); the slope of the line yields the wave speed  $c$ . The inset shows the dependence of  $c$  on the layer depth  $h$ . The curve is given by shallow water theory,  $c = \sqrt{gh}$ . The error includes uncertainty in the depth due to leveling of the container (horizontal error bars) and uncertainty in the algorithm determining the angle (vertical error bars).

free surface patterns [21]. When the depth of a fluid is small compared to the other dimensions in the system, one can neglect the fluid velocity in the vertical direction compared with the velocity components parallel to the surface. In this shallow water approximation, the equations describing the motion of a free surface of an incompressible, isothermal fluid in a gravitational field have the same form as the equations for a compressible gas flow [22]. In both cases a shock forms when the relative velocity between the fluid and the obstacle is greater than a critical velocity. For waves on a free surface the critical velocity is the maximum gravitational wave speed,  $c = \sqrt{gh}$ , for long waves without surface tension, and the shock is a discontinuity in height. Our measurements for different layer depths yield surface wave speeds in accord with the shallow water interpretation (inset to Fig. 3).

The agreement with shallow water theory for layer depths as small as one particle diameter is surprising. A vibrated granular layer is highly compressible [6, 13]; during each collision with the plate, a shock wave forms in the bulk of the fluid and travels through the layer, compressing and heating the grains. Although the volume fraction can change by a factor of two and the granular temperature across the shock can increase by two orders of magnitude [13], the energy is quickly dissipated by inelastic collisions [23, 24]. Our molecular dynamics simulations for the conditions of our experiment show that throughout much of the cycle the bulk of the layer has an approximately constant density and temperature. The forcing of the plate acts only to fluidize the granular

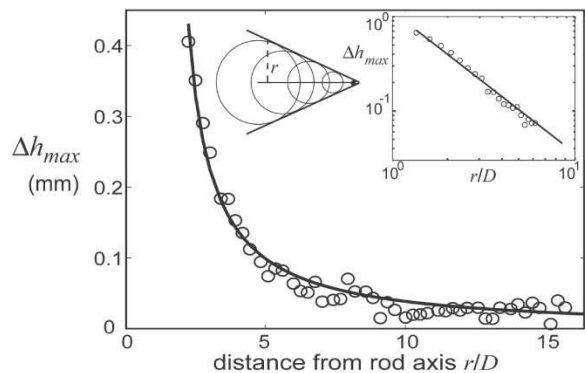


FIG. 4: The maximum height of the shock front as a function of  $r$ , the perpendicular distance to the shock from the rod's axis of motion. The shock formed by the coalescence of cylindrical waves (inset) does not extend into the fluid indefinitely, but decays as  $r^{-3/2}$  (solid curve), as predicted by the Landau theory. The line in the log-log plot (inset) has slope  $-3/2$

layer and does not play a strong role in the propagation of waves on the surface. We expect the shock front in a shallow granular layer to be unchanged under different methods for fluidization.

*Shock decay.* We find the granular shock rapidly decreases in intensity as it propagates into the surrounding fluid. The decay of  $\Delta h_{max}$  of the shock versus  $r$ , the distance from the shock to the axis of motion of the rod, is plotted in Fig. 4. The functional form of the decay agrees with scaling predictions by Landau [25] for discontinuities in cylindrical sound waves propagating into a dissipationless fluid. The velocity of each point in the shock front  $u$  can be approximated by  $u = c_0 + (\partial u / \partial \rho)_S (\rho_0 v_0 / c_0) \sqrt{r_0 / r}$ , where  $c_0$  is the wave speed of the undistorted front,  $(\partial u / \partial \rho)_S$  describes the adiabatic variation of wave speed with the local density, and  $v_0 \sqrt{r_0 / r}$  accounts for the decrease in the intensity of a cylindrical wave as it propagates away from its point of origin. Conservation of mass requires the area of a shock profile remains constant as it moves. As the intensity of the shock decays, the width of the shock increases. Setting the areas of shock profiles separated by a time  $\Delta t$  equal, Landau found that the width of the shock increases as  $r^{1/4}$ , where  $r$  is the distance from the shock to the axis of motion of the rod (inset of Fig. 4), and the shock intensity  $\Delta v$  decreases as  $r^{-3/4}$ . For a shallow fluid,  $\Delta v \propto \sqrt{\Delta h}$ , implying  $\Delta h$  should decay as  $r^{-3/2}$ . The solid line in Fig. 4 is a fit to  $\Delta h_{max}$  proportional to  $r^{-3/2}$ .

*Conclusions:* Our experiments demonstrate that a thin vertically vibrated granular layer is described well by shallow water theory for a surface-tensionless fluid. We find that a shock forms on the surface when an obstacle's velocity exceeds the speed of a gravity wave,  $c = \sqrt{gh}$ . The angle of the shock cone is determined by the Mach relation, and the damping of the shock follows the scaling

derived by Landau for shocks traveling in a dissipationless fluid. Future experiments should study the applicability of this model as a function of layer depth and inelasticity. For deeper layers, the shock generated when the layer collides with the bottom plate may not travel to top of the layer [24], possibly changing the behavior.

The shocks formed in our experiment are an example of Cerenkov radiation generated by an object traveling through a medium faster than the wave phase velocity [26]. Such radiation leads to increased resistance (wave drag) when a critical velocity is exceeded. Future experiments should examine the dependence of drag on  $v_R$  near the onset of the shock because experiments [27, 28], simulations [9, 11], and theory [29, 30] disagree on this increase in drag.

We thank Jon Bougie, Robert Deegan, W.D. McCormick, Larsson Omberg, Jack Swift and Paul Umbanhowar for helpful discussions. This research was supported by the Engineering Research Program of the Office of Basic Energy Science of the U.S. Department of Energy (Grant No. DE-FG03-93ER14312), by The Texas Advanced Research Program (Grant No. ARP-055-2001), and by the Office of Naval Research Quantum Optics Initiative (Grant No. N00014-03-1-0639).

- 
- [1] D. Tritton, *Physical Fluid Dynamics* (Oxford University Press, New York, 1988).
  - [2] P. K. Haff, *J. Fluid Mech.* **134**, 401 (1983).
  - [3] G. Ahmadi and M. Shahinpoor, *Int. J. Non-linear Mechanics* **19**, 177 (1983).
  - [4] C. K. K. Lun, *J. Appl. Mech.* **54**, 47 (1987).
  - [5] J. T. Jenkins and M. W. Richman, *Arch. Rat. Mech. Anal.* **87**, 355 (1985).
  - [6] A. Goldshtein and M. Shapiro, *J. Fluid Mech.* **282**, 75 (1995).
  - [7] N. Sela, I. Goldhirsch, and S. H. Noskowitz, *Phys. Fluids* **8**, 2337 (1996).
  - [8] J. J. Brey, J. W. Dufty, and A. Santos, *J. Stat. Phys.* **87**, 1051 (1997).
  - [9] C. Wassgren, J. Cordova, R. Zenit, and A. Karion, *Phys. Fluids* **15**, 3318 (2003).
  - [10] M.-L. Tan and I. Goldhirsch, *Phys. Rev. Lett.* **81**, 3022 (1998).
  - [11] V. Buchholtz and T. Pöschel, *Granular Matter* **1**, 33 (1998).
  - [12] E. C. Rericha, C. Bizon, M. D. Shattuck, and H. L. Swinney, *Phys. Rev. Lett.* **88**, 014302 (2002).
  - [13] J. Bougie, S. J. Moon, J. B. Swift, and H. L. Swinney, *Phys. Rev. E* **66**, 051301 (2002).
  - [14] F. Melo, P. Umbanhowar, and H. L. Swinney, *Phys. Rev. Lett.* **72**, 172 (1994).
  - [15] D. I. Goldman, J. B. Swift, and H. L. Swinney, *Phys. Rev. Lett.* **92**, 174302 (2004).
  - [16] N. Mujica and F. Melo, *Phys. Rev. Lett.* **80**, 5121 (1998).
  - [17] H. K. Pak, E. Van Doorn, and R. P. Behringer, *Phys. Rev. Lett.* **74**, 4643 (1995).
  - [18] Y. Forterre and O. Pouliquen, *Phys. Rev. Lett.* **86**, 5886 (2001).
  - [19] S. Savage and K. Hutter, *Acta Mechanica* **86**, 201 (1991).
  - [20] J. Gray, Y. Tai, and S. Noelle, *J. Fluid Mech.* **491**, 161 (2003).
  - [21] C. Bizon, M. D. Shattuck, and J. B. Swift, *Phys. Rev. E* **60**, 7210 (1999).
  - [22] L. Landau and E. Lifshitz, *Fluid Mechanics* (Pergamon Press, Oxford, 1959).
  - [23] C. Bizon, M. D. Shattuck, J. B. Swift, W. D. McCormick, and H. L. Swinney, *Phys. Rev. Lett.* **80**, 57 (1998).
  - [24] A. Goldshtein, A. Alexeev, and M. Shapiro, in *Granular Gas Dynamics*, edited by T. Poschel and N. Brilliantov (Springer, Berlin, 2003), pp. 188–225.
  - [25] L. Landau, in *Collected Papers of L.D. Landau*, edited by D. T. Haar (Pergamon Press, 1965), pp. 437–444.
  - [26] J. V. Jelley, *Cerenkov Radiation and Its Applications* (Pergamon Press, New York, 1958).
  - [27] O. Zik, J. Stavans, and Y. Rabin, *Europhys. Lett.* **17**, 315 (1992).
  - [28] T. Burghlea and V. Steinberg, *Phys. Rev. Lett.* **86**, 2557 (2001).
  - [29] E. Raphaël and P.-G. de Gennes, *Phys. Rev. E* **53**, 3448 (1996).
  - [30] F. Chevy and E. Raphaël, *Europhys. Lett.* **61**, 796 (2003).
  - [31] Uncertainties in our experimental determination of the critical velocity  $c$  are due to the subjective choice of the interval for the linear fits (dashed line in Fig. 2 and blue lines in Fig. 1(b)). Uncertainties in the layer depth  $h$  are due to leveling of the container.